

A spectral element analysis of sound transmission through metallic sandwich plates with adhesively-bonded corrugated cores

Hao Sen Yang¹, Heow Pueh Lee^{2,*}, Hui Zheng^{1,**}

¹ Institute of Vibration, Shock & Noise, School of Mechanical Engineering
Shanghai Jiao Tong University, 800 Dongchuan Road, Shanghai 200240, China.

²Department of Mechanical Engineering, The National University of Singapore
9 Engineering Drive 1, Singapore 117575

*Presenting author: mpeleehp@nus.edu.sg

**Corresponding author: huizheng@sjtu.edu.cn

Abstract

This paper presents a spectral element based numerical method for calculating the vibro-acoustic response of sandwich plates with adhesively-bonded corrugated cores. The study is motivated by the need of optimal designs for improving the structural-acoustic performance of the considered structures. A two-dimensional plate model is firstly developed based on the spectral element method (SEM) for obtaining the frequency-domain vibration response of the whole structure subject to incident harmonic acoustic wave. Thereafter the Rayleigh integral formula is used to calculate the transmitted sound power via its structure-borne path. Comparing with the conventional finite element method, the SEM, since it is formulated in the frequency domain by using the exact wave solutions for the governing differential equation, provides exact frequency-domain solutions meanwhile using much fewer number of degrees-of-freedom. This is proven by the numerical results of structural vibration response. Furthermore, parametric studies are performed to investigate the influence of the inclined angle of bonded corrugated core and the thickness of face plates on the transmitted sound power of sandwich plates. Although these design parameters have different effects on the sound transmission loss in different frequency-bands of interest, the impacts of both of them become more evident with the increase of targeted sound-insulating frequency.

Keywords: Sandwich plate; corrugated core; spectral element; Sound transmission.

Introduction

Metallic sandwich plates with corrugated cores are used extensively in the high speed transportation engineering field for their lower area density, higher specific strength and stiffness than those of a homogeneous type. Vibro-acoustic response of this kind of structures subject to airborne excitation have been a concern in acoustic comfort design of high speed transportation systems such as airplanes and express trains.

Considering the wide usage of the sandwich structure, various theoretical studies have been performed aiming at understanding the mechanism of sound transmission through such kind of structure. The early studies of acoustic radiation problem for periodic stiffened structure are limited to single beam or plate[1–3], and the main concern of these works is the vibro-acoustic response of periodic stiffened structure under mechanical forces. For the double layer structure, starting from the double-leaf partitions made up of homogeneous panels with no structural stiffener in the core, Pellicier and Trompette[4] reviewed various wave approach based methods for calculating the partitions transmission loss, and proposed a simple mechanism on the theory of sound transmission through such kind of structure. Considering the stiffened double layer structure, Wang et al.[5] studied the double-leaf lightweight partitions stiffened with periodically placed studs, and presented a theoretical model to predict the sound transmission loss of the structure. Legault et al.[6] studied the sound transmission

transmission of sandwich structures with cellular cores or truss-like periodic panels[10,16,17], the sandwich plate with corrugated core is assumed infinite along the z -axis. Thus the three-dimensional sandwich plates can be simplified a sandwich beam structure represented by the cross section as shown in Figure 1(b).

Spectral element method modeling

For spectral element method, the governing equation of motion of the global system is assembled by all the spectral elements, and it is given in the frequency-domain as

$$S_g(\omega)D_g(x, \omega) = F_g \quad (1)$$

where S_g , D_g and F_g represent the global dynamic stiffness matrix, the global spectral nodal DOFs vector, and the global nodal force vector, respectively. For beam structure, the exact dynamic stiffness matrix is formulated based on the exact wave solutions to the governing differential equations[18]. Thus, theoretically, SEM can provide accurate solution to the dynamic response of the beam structure, but, comparing to the conventional finite element method, SEM only uses a minimum number of DOFs, which makes SEM much more computationally efficient[19].

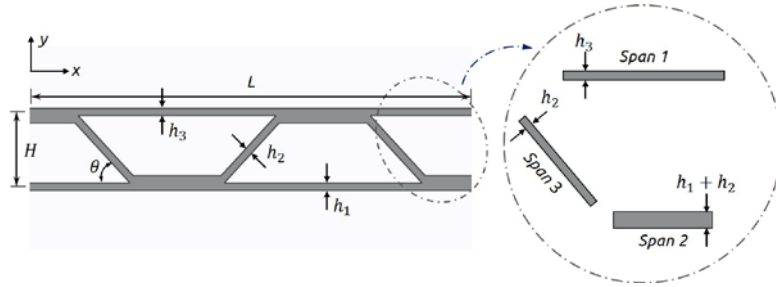


Figure. 2 Geometric configuration of sandwich beam

Figure. 2 gives the details of the sandwich beam with a finite total length of L and total height of H . h_1 , h_2 and h_3 represent the thickness of the lower face plate, core plate and the upper face plate. The inclined angle of the stiffened core is defined as θ . Both the face plates and core are made of the same isotropic, homogeneous material with the elasticity modulus E and density ρ . In order to apply the spectral element method, the sandwich beam structure is firstly divided into a number of spans, and each span can be treated as a single spectral element.

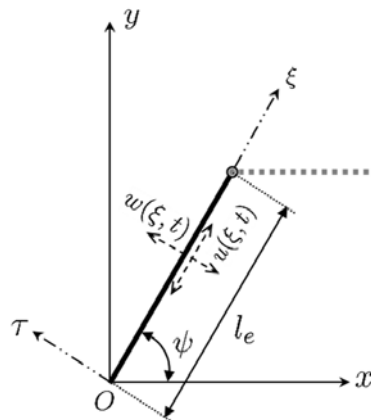


Figure. 3 Local & global coordinate system of a beam element

An illustration of a single spectral beam element in the local coordinates system is shown in Figure 3, the classical governing equations of free longitudinal and flexural vibration are:

$$\frac{\partial^2 u(\xi, t)}{\partial \xi^2} - \frac{\rho}{E} \cdot \frac{\partial^2 u(\xi, t)}{\partial t^2} = 0, \quad \frac{\partial^4 w(\xi, t)}{\partial \xi^4} + \frac{\rho A}{EI} \cdot \frac{\partial^2 w(\xi, t)}{\partial t^2} = 0 \quad (2)$$

where $u(\xi, t)$, $w(\xi, t)$ are respectively, the longitudinal and flexural displacement in the local coordinate system. A is the cross-sectional area, I is the cross sectional moment of inertia. The solution to Eq. (2) is assumed in the spectral form as:

$$u(\xi, t) = \frac{1}{N} \sum_{n=1}^N U_n(\xi; \omega_n) \cdot e^{i\omega_n t}, \quad w(\xi, t) = \frac{1}{N} \sum_{n=1}^N W_n(\xi; \omega_n) \cdot e^{i\omega_n t} \quad (3)$$

at a specific discretization frequency $\omega = \omega_n$, the general solution to Eq. (2) can be written as:

$$\begin{cases} U_n(\xi; \omega_n) = \{e^{-ik_l \xi} & e^{+ik_l \xi}\} \cdot \{C_l\}, & k_l = \omega_n \sqrt{\rho/E} \\ W_n(\xi; \omega_n) = \{e^{ik_f \xi} & e^{-ik_f \xi} & e^{-k_f \xi} & e^{k_f \xi}\} \cdot \{C_f\}, & k_f = \sqrt[4]{\rho A \omega_n^2 / EI} \end{cases} \quad (4)$$

where $\{C_l\}$ and $\{C_f\}$ are both constant column vectors. The longitudinal and transverse nodal displacement at both ends of the beam element can be written as:

$$\begin{cases} \mathbf{d}_l = \{u_1|_{\xi=0} & u_2|_{\xi=l_e}\} = \mathbf{B}_l \cdot \{C_l\} \\ \mathbf{d}_f = \{w_1|_{\xi=0} & \theta_1|_{\xi=0} & w_2|_{\xi=l_e} & \theta_2|_{\xi=l_e}\} = \mathbf{B}_f \cdot \{C_f\} \end{cases} \quad (5)$$

u , w and θ are, respectively, longitudinal displacement, deflection and slope. Considering the force-displacement relation, the internal axial force $F(\xi)$, shear force $T(\xi)$ and moment $M(\xi)$ are given by:

$$F(\xi) = EA \frac{dU(\xi)}{d\xi}, \quad T(\xi) = -EI \frac{d^3 W(\xi)}{d\xi^3}, \quad M(\xi) = EI \frac{d^2 W(\xi)}{d\xi^2} \quad (6)$$

According to the compatibility condition, using Eq. (4) and Eq. (6), the external spectral nodal forces and moments acting on the two nodes of the beam element can be given as the form of:

$$\mathbf{f}_l = \{\tilde{F}_1 \quad \tilde{F}_2\}^T = \mathbf{H}_l \cdot \{C_l\}, \quad \mathbf{f}_f = \{\tilde{T}_1 \quad \tilde{M}_1 \quad \tilde{T}_2 \quad \tilde{M}_2\}^T = \mathbf{H}_f \cdot \{C_f\} \quad (7)$$

Eliminate the constant vectors using Eq. (5) and Eq. (7), it gives:

$$\underbrace{\mathbf{H}_l \cdot \mathbf{B}_l^{-1}}_{\mathbf{S}_l(\omega_n)} \cdot \mathbf{d}_l = \begin{bmatrix} \kappa_{11}^L & \kappa_{12}^L \\ \kappa_{21}^L & \kappa_{22}^L \end{bmatrix} \cdot \mathbf{d}_l = \mathbf{f}_l, \quad \underbrace{\mathbf{H}_f \cdot \mathbf{B}_f^{-1}}_{\mathbf{S}_f(\omega_n)} \cdot \mathbf{d}_f = \begin{bmatrix} \kappa_{11}^F & \kappa_{12}^F & \kappa_{13}^F & \kappa_{14}^F \\ \kappa_{21}^F & \kappa_{22}^F & \kappa_{23}^F & \kappa_{24}^F \\ \kappa_{31}^F & \kappa_{32}^F & \kappa_{33}^F & \kappa_{34}^F \\ \kappa_{41}^F & \kappa_{42}^F & \kappa_{43}^F & \kappa_{44}^F \end{bmatrix} \cdot \mathbf{d}_f = \mathbf{f}_f \quad (8)$$

where $\mathbf{S}_l(\omega_n)$ and $\mathbf{S}_f(\omega_n)$ are known as spectral element matrix for longitudinal and transvers vibration of a single beam element. Combining the longitudinal and transvers equation into one single spectral equation, it gives:

$$\underbrace{\begin{bmatrix} \kappa_{11}^L & 0 & 0 & \kappa_{12}^L & 0 & 0 \\ 0 & \kappa_{11}^F & \kappa_{12}^F & 0 & \kappa_{13}^F & \kappa_{14}^F \\ 0 & \kappa_{21}^F & \kappa_{22}^F & 0 & \kappa_{23}^F & \kappa_{24}^F \\ \kappa_{21}^L & 0 & 0 & \kappa_{22}^L & 0 & 0 \\ 0 & \kappa_{31}^F & \kappa_{32}^F & 0 & \kappa_{33}^F & \kappa_{34}^F \\ 0 & \kappa_{41}^F & \kappa_{42}^F & 0 & \kappa_{43}^F & \kappa_{44}^F \end{bmatrix}}_{\mathbf{S}(\omega_n)} \underbrace{\begin{bmatrix} u_1 \\ w_1 \\ \theta_1 \\ u_2 \\ w_2 \\ \theta_2 \end{bmatrix}}_{\mathbf{d}} = \mathbf{f} = \begin{bmatrix} \widetilde{F}_1 \\ \widetilde{T}_1 \\ \widetilde{M}_1 \\ \widetilde{F}_2 \\ \widetilde{T}_2 \\ \widetilde{M}_2 \end{bmatrix} \quad (9)$$

where $\mathbf{S}(\omega_n)$ is the general spectral element matrix of a single beam. The continuous displacement field can be represented by the spectral nodal displacements \mathbf{d} as

$$\mathbf{G}(\xi) = \widetilde{\mathbf{N}} \cdot \mathbf{d} \quad (10)$$

$\mathbf{G}(\xi)$ represents both the longitudinal and flexural displacements, and $\widetilde{\mathbf{N}}$ is the dynamic shape function which can be obtained from Eq. (4) and Eq. (5). When the structure is exposed to a distributed force loading, the distributed force $\mathbf{P}(\xi, \omega_n)$ must be transferred to each node of the spectral elements by using the virtual work principle in the frequency-domain.

$$\mathbf{f} = \int_0^{l_e} \widetilde{\mathbf{N}}^T(\xi, \omega_n) \mathbf{P}(\xi, \omega_n) d\xi \quad (11)$$

Now the governing equation of motion of a single spectral element can be symbolically represented by

$$\mathbf{s}(\omega_n)_{local} \cdot \mathbf{d}_{local} = \mathbf{f}_{local} \quad (12)$$

With the coordinate transformation matrix \mathbf{T} :

$$\mathbf{d}_{global} = \mathbf{T} \cdot \mathbf{d}_{local}, \quad \mathbf{f}_{global}^d = \mathbf{T} \cdot \mathbf{f}_{local}^d, \quad \mathbf{s}(\omega)_{global} = \mathbf{T}^{-1} \cdot \mathbf{s}(\omega)_{local} \cdot \mathbf{T} \quad (13)$$

The spectral equations of the whole sandwich structure can be written as the assembly of the coordinate transformed local equations:

$$\mathbb{S}(\omega_n) \cdot \mathbb{D} = \mathbb{F} \quad (14)$$

Acoustic radiation

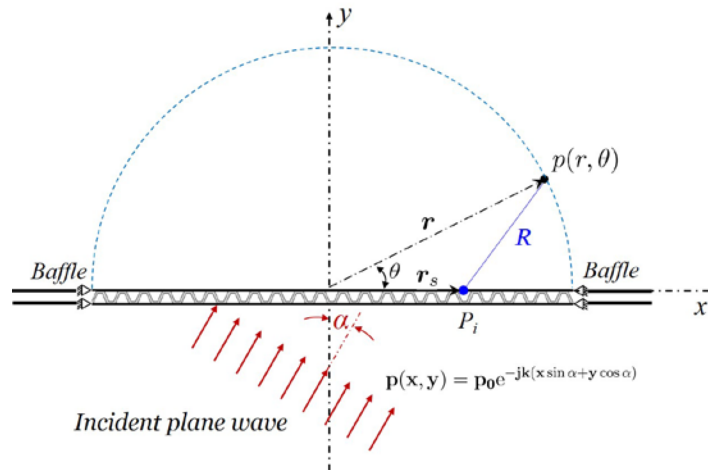


Figure 4. The acoustic transmission model

It is assumed that the sandwich beam is baffled at both the top and bottom surface, as shown in Figure 4. Considering a unit magnitude acoustic plane wave impinged on the bottom beam surface with an incident angle of α . The acoustic pressure is transmitted to the top beam via the structure-borne path and radiates sound to the semi-infinite space. The half-circle illustrated in Figure 4 is the observation surface where the acoustic power radiated from the top beam surface is calculated.

The transmitted acoustic pressure $p(r, \theta, \omega)$ at a specific observation point \mathbf{r} due to the surface normal velocity v_i on the top beam can be calculated using the Rayleigh's integral[20]:

$$p(\mathbf{r}, \theta, \omega) = \int_L \frac{\rho_0 \omega}{2} H_0^{(2)} [kR(x)] \cdot v(x) dx \quad (15)$$

where ρ_0 is the air density, $R = |\mathbf{r} - \mathbf{r}_s|$ and $H_0^{(2)}$ is the Hankel function of the second kind. The acoustic power radiated from the baffled beam at frequency ω can be obtained by an integration over the receiver surface (the half round surface S' shown in Figure 4):

$$W(\omega) = \frac{1}{2\rho_0 c_0} \cdot \int_{S'} p^2(r, \theta, \omega) \cdot r \, d\theta \quad (16)$$

Numerical validation

To verify the accuracy of present spectral element method, both the conventional FEM and SEM are used to calculate the vibration response of the sandwich beam structure. The structural drawing of the validation model has been given in Figure 3, in order to be more rigorous, two sets of design parameters are chosen to test the present method. The details of the two models are listed in Table 1. Another is worth mentioning, the whole structure is made of aluminum, with the modulus of elasticity is 7.1×10^{10} Pa, structural damping factor is 0.01, and the mass density is 2700 kg/m³.

Table 1. Validation model parameters

Parameter	Model 1	Model 2
Total length of the sandwich structure (L)	1200.0 mm	
Total height of the sandwich beam (H)	50.0 mm	
Number of inclined stiffener (N)	11	
Inclined angle of the stiffener (θ)	40°	60°
Thickness of the top face beam (h_3)	2.0 mm	
Thickness of the bottom face beam (h_1)	2.0 mm	
Thickness of the core beam (h_2)	2.0 mm	

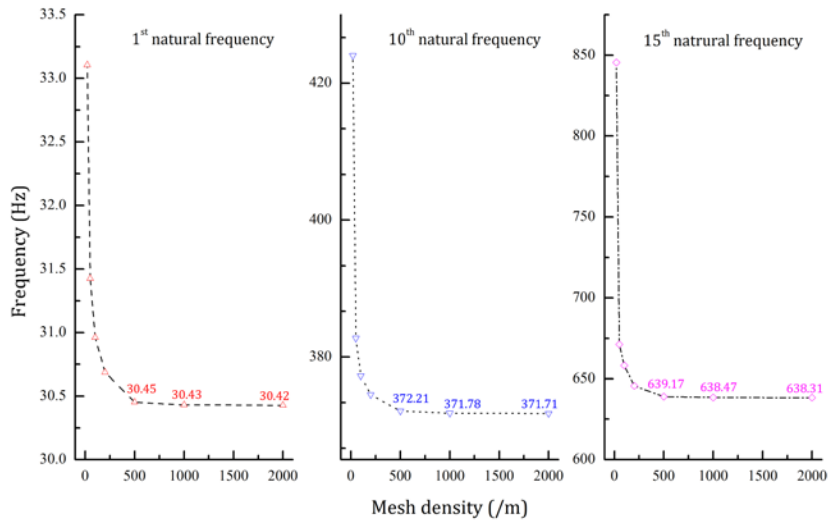


Figure 5. FEM mesh convergency

To ensure the reliability of the FEM results, a mesh convergency study is performed based on model 2 given in Table 1. The mesh convergency diagram is shown in Figure 6, the 1st, 10th and 15th natural frequency of the sandwich structure are chosen to be criteria of the convergency study. As shown in Figure 5, high frequency analysis requires high mesh density, in consideration of the computational efficiency, under 1000Hz, the mesh density of 1000/m is chosen to perform the FEM harmonic analysis.

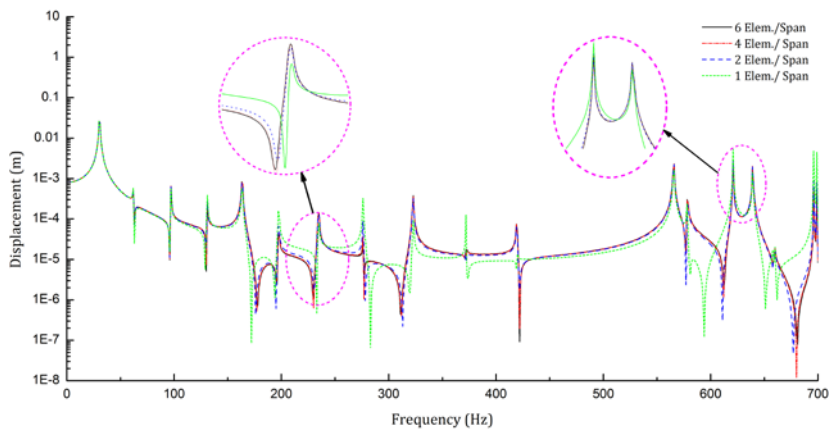
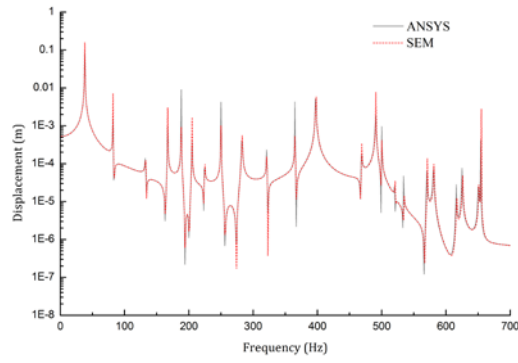


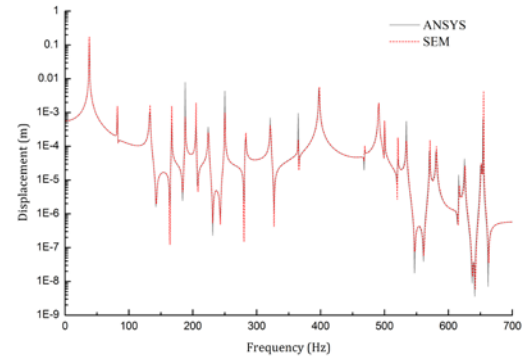
Figure 6. SEM element convergency

As for the present spectral element method, the convergency study is also performed as shown in Figure 6, the test model is also model 2 given in Table 1 and the observation point is located at $1/3 L$ of the top beam. The results indicate that when the element density is bigger than $2/\text{span}$, the difference between the curves of the dynamic response is quite small, thus, the element density of $4/\text{span}$ is used in this paper which is much smaller than the FEM.

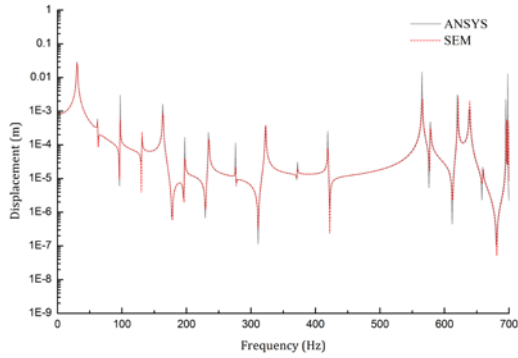
Considering a uniform distributed acoustic pressure with a unit magnitude is acting on the whole bottom beam surface, and the simply supported boundary conditions are applied at both ends of the top and bottom beams. The displacement response of two observation points, respectively, located at $1/3L$ and $1/2L$ of the top beam are given in Figure 7.



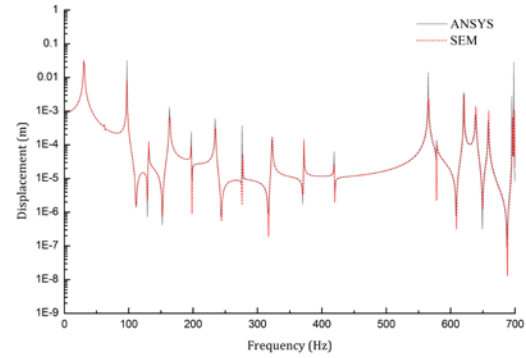
(a) model 1, point $1/3 L$



(b) model 1, point $1/2 L$



(c) model 2, point $1/3 L$



(d) model 2, point $1/2 L$

Figure 7. Point displacement of the validation model

According to Figure 7, the numerical results of present SEM agree very well with the results provided by the conventional FEM. It should be emphasized that when SEM is used to compute the vibration response of the validation model, a single computational run takes 21.7 seconds only. Comparing with 401.3 seconds of FEM, SEM uses only 5.4% computational time of the conventional FEM to obtain the same accurate results.

Parametric study

Benefit from the computational time and accuracy of present spectral element method, the vibration response of the sandwich structure subject to external sound wave excitation with wide frequency range can be calculated more effectively. Furthermore, by using the Rayleigh's integral, as given by Eq. (18), the transmitted sound power can be easily obtained. To provide a reference for the structural-acoustical design of the sandwich structure with adhesively-bonded corrugated cores given in this paper, parametric studies are implemented to reveal the effect of the thickness of the face plates and the inclined angle of stiffener on the transmitted sound power. The details of the reference model for the parametric study is tabulated in Table 2.

Table 2. Reference model for parametric study

Parameter	value
Total length of the sandwich structure (L)	1200.0 mm
Total height of the sandwich beam (H)	50.0 mm

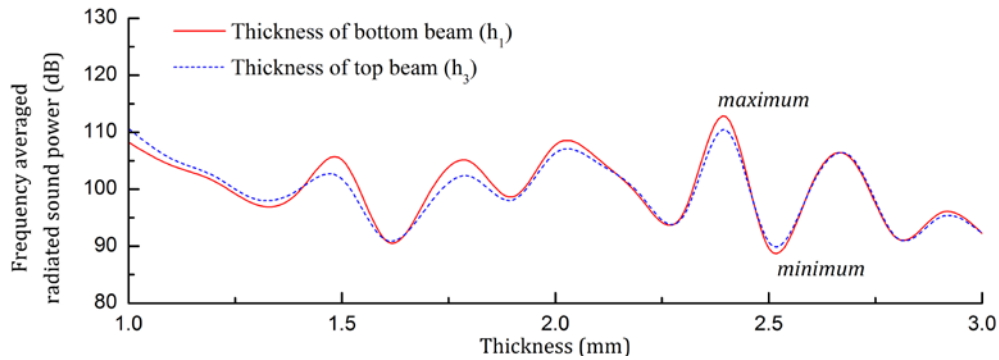
Number of inclined stiffener (N)	11
Inclined angle of the stiffener (θ)	Variate, $30^\circ \sim 90^\circ$
Thickness of the top face beam (h_3)	Variate, 1.0 ~ 3.0 mm
Thickness of the bottom face beam (h_1)	Variate, 1.0 ~ 3.0 mm
Thickness of the core beam (h_2)	3.0 mm

As illustrated in Figure 4, considering a unit magnitude plane wave of acoustic pressure is impinging on the bottom beam surface with an incident angle of $\alpha=30^\circ$. The frequency range of the excitation is 1~800Hz, and the frequency averaged sound power is introduced here as an evaluation index for the acoustic performance of the sandwich structure, which is:

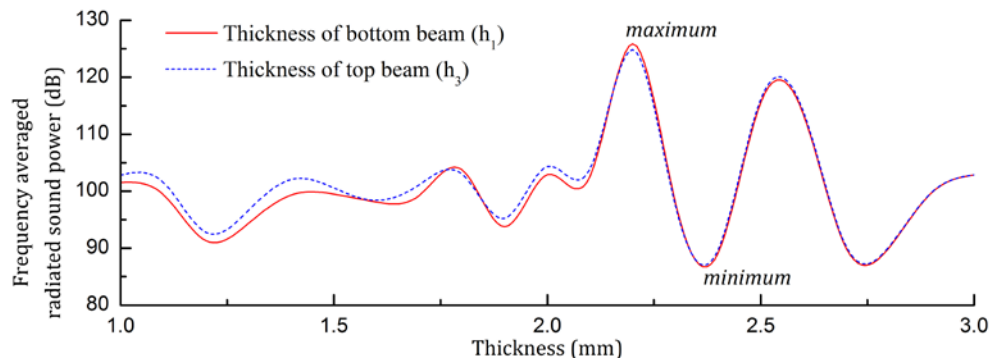
$$W_a = \frac{1}{\omega_2 - \omega_1} \int_{\omega_1}^{\omega_2} W(\omega) d\omega \quad (18)$$

Effect of the thickness of the face plate

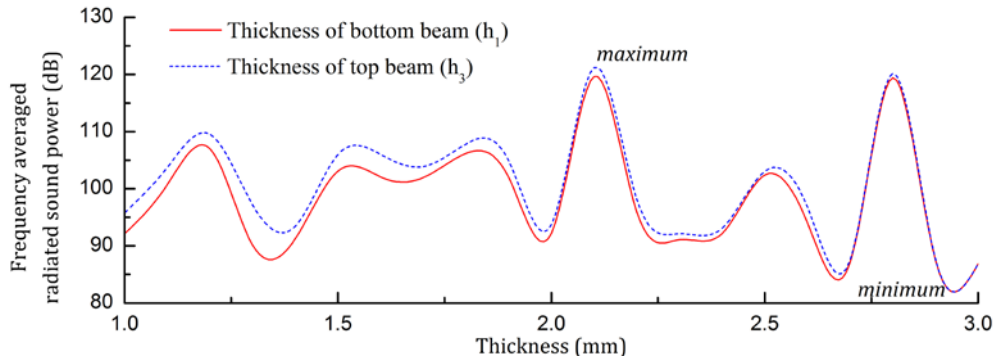
Figure 8 gives the effect of the thickness of the face plates on the radiated sound power with the target frequency range from 0 to 800Hz. As is shown in the graph, for the univariate study, because of the periodicity of the sandwich structure, h_1 and h_3 affect the frequency averaged sound power in much the same way.



(a) Inclined angle of stiffener $\theta=30^\circ$



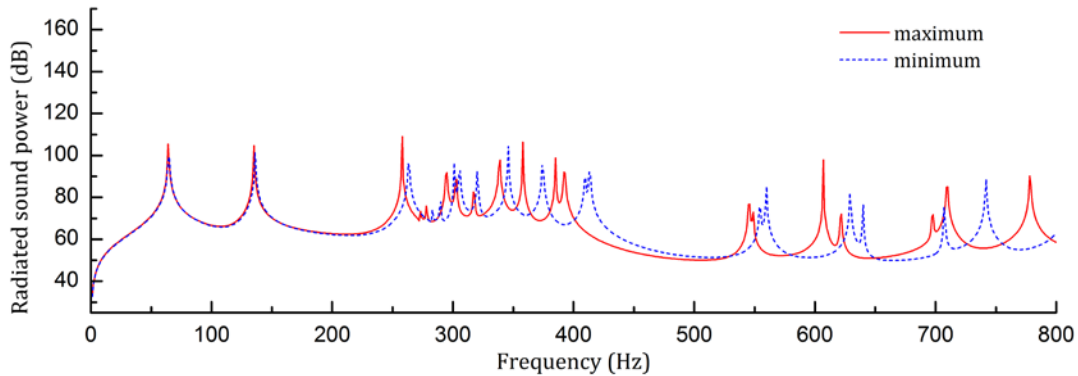
(b) Inclined angle of stiffener $\theta=40^\circ$



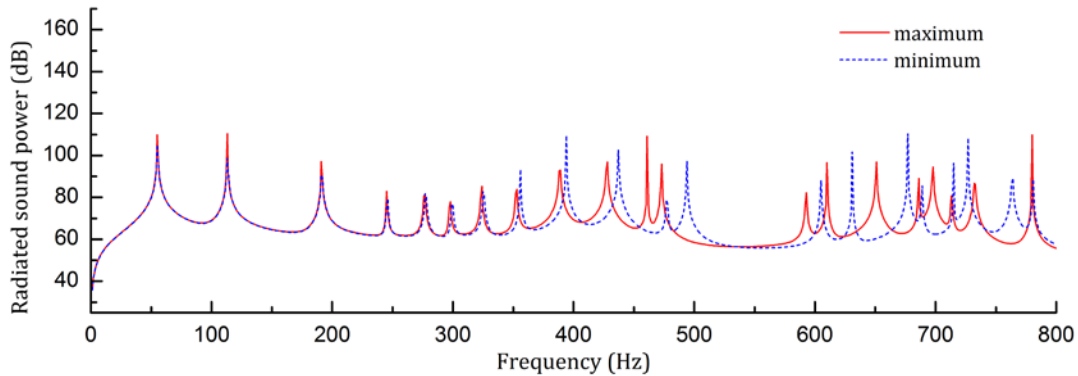
(c) Inclined angle of stiffener $\theta=50^\circ$

Figure 8. Influence of the thickness of the face plates

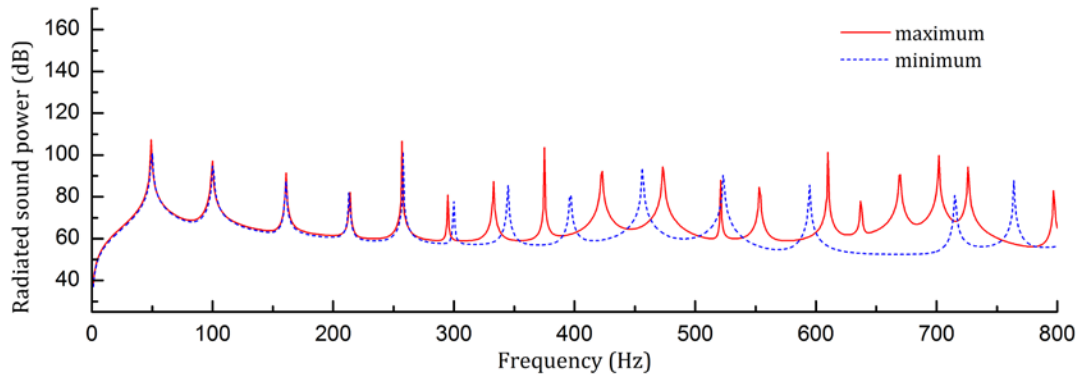
Just for one specific inclined angle, as the increase of the thickness, there are less differences between the two curves in each sub-figure, and also, the influence become more obvious and the variation tendency become more violent. The spectral distribution of structural radiated sound power of the maximum and minimum points in Figure 8 are plotted in Figure 9. It can be seen that the main difference between the maximum curve and minimum curve is in the high frequency range, the changing of the thickness of the face plates has a limited impact on the radiated sound power in the low frequency range.



(a) Inclined angle of stiffener $\theta=30^\circ$



(b) Inclined angle of stiffener $\theta=40^\circ$



(c) Inclined angle of stiffener $\theta=50^\circ$

Figure 9. Spectral distribution of the radiated sound power of the maximum and minimum point in Figure 8

Effect of inclined angle θ

By fixing both the thickness of the top and bottom beam at 3mm, the effect of the inclined angle of the stiffener is illustrated in Figure 10. In order to avoid the interference between two adjacent stiffeners, the variation range of the inclined angle is limited from 30 to 90 degrees.

Due to the structural inhomogeneity of the adhesively-bonded corrugated core layer, as there is any change of the inclined angle, not only the structure layout, but also the structural mass and stiffness are changed simultaneously. These complex relationships eventually lead to an erratic curve as shown in Figure 10 with the target frequency range from 0 to 500Hz.

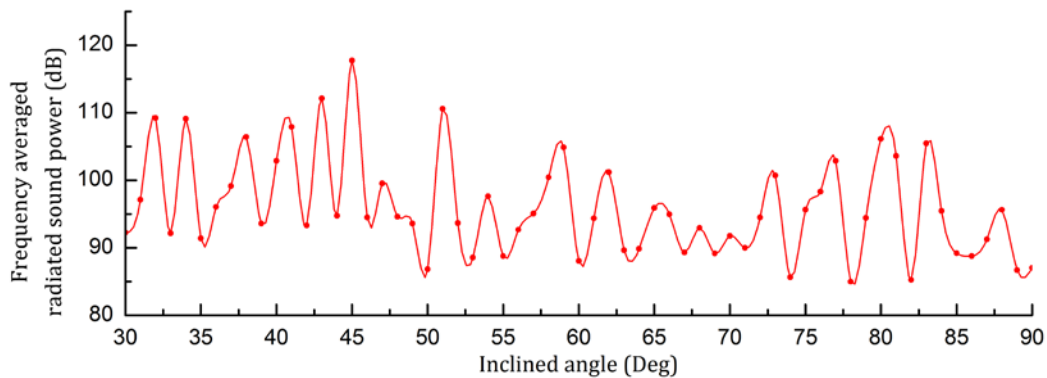


Figure 10. Influence of the incline angle of the stiffener

Since h_1 and h_3 have the same effect on the radiated sound power, either one could be used to perform the thickness and angle combined influence study on the radiated sound power. As shown in Figure 11, in zone 1, with big thickness and less inclination of the stiffeners, the change tendency of the sound power is relatively gently. To the contrary, in zone 2, small thickness and small inclined angle lead to less structural stiffness and dramatic fluctuation of sound power in this zone.

According to the data of Figure 11, the maximum and minimum value are 128.8dB and 89.1dB, which appear when $h_1=2.0\text{mm}$, $\theta=87^\circ$ and $h_1=1.5\text{mm}$, $\theta=84^\circ$, respectively. The spectral distribution of radiated sound power is given in Figure 12, obviously, the main difference between the two curves is high frequency range. In fact, for the sandwich structure, the sound radiation in low frequency range gives the greatest contribution to the averaged radiated sound power and it is hard to control.

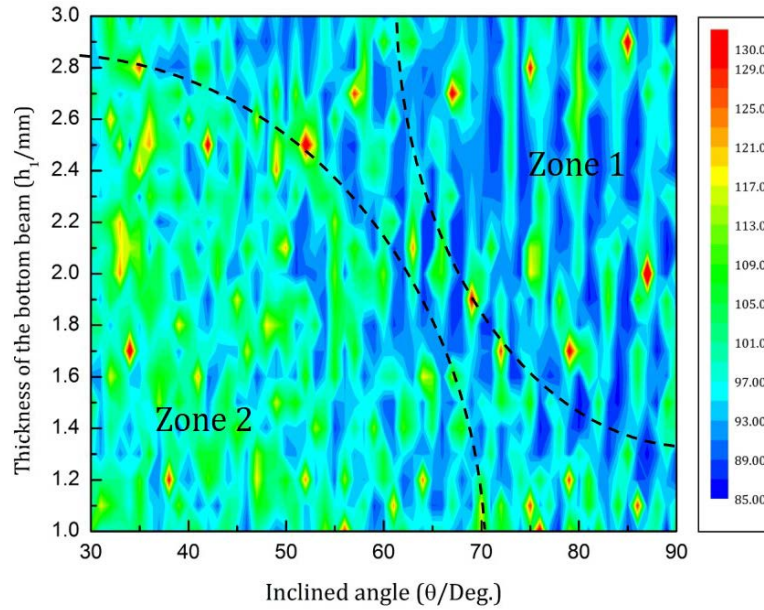


Figure 11. Frequency averaged sound power related to both the thickness of the face plate and the inclined angle of the stiffener

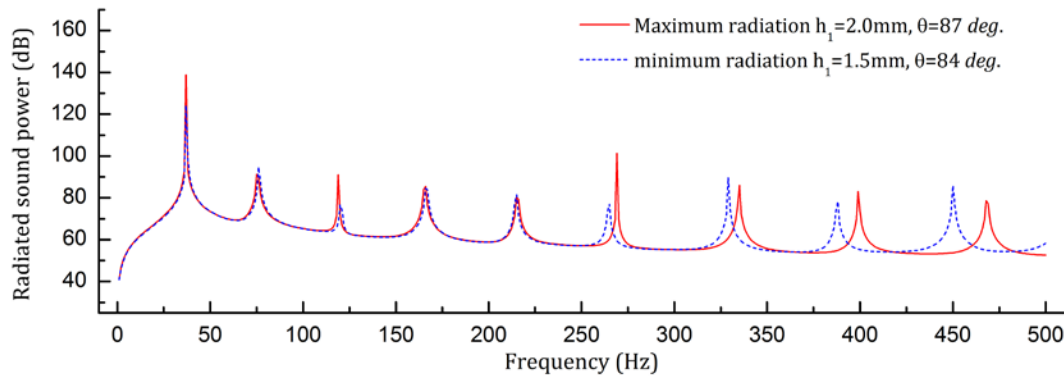


Figure 12. Spectral distribution of the radiated sound power

Conclusions

In this paper, a finite-length numerical 2D model of sandwich plates with adhesively-bonded corrugated cores is developed using spectral element method. The numerical result shows that SEM has a much higher computational efficiency than the traditional FEM without losing any accuracy, which makes SEM an efficient method for the vibro-acoustic analysis of such periodic structure. By using the Rayleigh's integral, parametric studies are performed to test the influence of two main design parameters, the thickness of the face plates and the inclined angle of the stiffener, on the radiated sound power when the structure is subjected to external sound wave excitation. The result shows that for the periodic structure, both the thickness of the top and bottom beam have almost the same effect on the frequency averaged radiation sound power. Comparing with the thickness of the face plates, the averaged sound power is more sensitive to the inclined angle of the stiffener. From the perspective of reducing the radiated sound power, the sound radiation in high frequency range can be affected more easily by changing these two parameters. Since the sound radiation in low frequency range gives the greatest contribution to the averaged radiated sound power, suppressing the sound radiation in low frequency range would be more important to reduce sound radiation of the whole structure.

Acknowledgments

This research is supported by the National Science Foundation of China (Grant No. 51275289).

References

- [1] Rumerman, M. L., 1975, "Vibration and wave propagation in ribbed plates," *J. Acoust. Soc. Am.*, **57**(2), pp. 370–373.
- [2] Mace, B. R., 1980, "Sound radiation from a plate reinforced by two sets of parallel stiffeners," *J. Sound Vib.*, **71**(3), pp. 435–441.
- [3] Mead, D. M., 1996, "Wave Propagation in Continuous Periodic Structures: Research Contributions From Southampton, 1964-1995," *J. Sound Vib.*, **190**(3), pp. 495–524.
- [4] Pellicier, A., and Trompette, N., 2007, "A review of analytical methods, based on the wave approach, to compute partitions transmission loss," *Appl. Acoust.*, **68**(10), pp. 1192–1212.
- [5] Wang, J., Lu, T. J., Woodhouse, J., Langley, R. S., and Evans, J., 2005, "Sound transmission through lightweight double-leaf partitions: Theoretical modelling," *J. Sound Vib.*, **286**(4-5), pp. 817–847.
- [6] Legault, J., and Atalla, N., 2010, "Sound transmission through a double panel structure periodically coupled with vibration insulators," *J. Sound Vib.*, **329**(15), pp. 3082–3100.
- [7] Xin, F. X., and Lu, T. J., 2011, "Transmission loss of orthogonally rib-stiffened double-panel structures with cavity absorption," *J. Acoust. Soc. Am.*, **129**(4), pp. 1919–34.
- [8] Thamburaj, P., and Sun, J. Q., 2002, "Optimization of Anisotropic Sandwich Beams for Higher Sound Transmission Loss," *J. Sound Vib.*, **254**(1), pp. 23–36.
- [9] Franco, F., Cunefare, K. a., and Ruzzene, M., 2007, "Structural-Acoustic Optimization of Sandwich Panels," *J. Vib. Acoust.*, **129**(3), p. 330.
- [10] Denli, H., and Sun, J. Q., 2007, "Structural-acoustic optimization of sandwich structures with cellular cores for minimum sound radiation," *J. Sound Vib.*, **301**(1-2), pp. 93–105.
- [11] Fahy, F., and Walker, J., 2004, *Advanced Applications in Acoustics, Noise and Vibration*, CRC Press, New York.
- [12] Patera, A. T., 1984, "A spectral element method for fluid dynamics: laminar flow in a channel expansion," *J. Comput. Phys.*, **54**, pp. 468–488.
- [13] Birgersson, F., Finnveden, S., and Nilsson, C. M., 2005, "A spectral super element for modelling of plate vibration. Part 1: General theory," *J. Sound Vib.*, **287**, pp. 297–314.
- [14] Zak, A., 2009, "A novel formulation of a spectral plate element for wave propagation in isotropic structures," *Finite Elem. Anal. Des.*, **45**(10), pp. 650–658.
- [15] Wu, Z., Li, F., and Wang, Y., 2013, "Study on vibration characteristics in periodic plate structures using the spectral element method," *Acta Mech.*, **1101**, pp. 1089–1101.
- [16] El-Raheb, M., and Wagner, P., 1997, "Transmission of sound across a trusslike periodic panel; 2-D analysis," *J. Acoust. Soc. Am.*, **102**(4), pp. 2176–2183.
- [17] Ruzzene, M., 2004, "Vibration and sound radiation of sandwich beams with

- honeycomb truss core,” *J. Sound Vib.*, **277**(4-5), pp. 741–763.
- [18] Lee, U., 2009, *Spectral Element Method in Structural Dynamics*, J. Wiley & Sons Asia, Hoboken, N.J.
- [19] Doyle, J. F., 1997, *Wave Propagation in Structures: Spectral Analysis Using Fast Discrete Fourier Transforms*, Springer, New York.
- [20] Fahy, F., and Gardonio, P., 2007, *Sound and Structural Vibration: Radiation, Transmission and Response*, Academic Press, London.